Dew-Point Loci for Methane–*n*-Hexane and Methane–*n*-Heptane Binary Systems

Roger J. J. Chen,[1] Patsy S. Chappelear,* and Riki Kobayashi*
Department of Chemical Engineering, William Marsh Rice University, Houston, Tex, 77001

The constant flow gas saturation technique developed in earlier studies of the methane–*n*-butane and methane–*n*-pentane systems was used for both systems reported here. Dew-point loci for the methane–*n*-hexane system were determined at eight temperatures from 0 to −82.65 °C, from 20 up to 2675 psia. Two liquid phases were observed, and detailed phase behavior was examined in the vicinity of the critical point of pure methane. Dew-point loci for the methane–*n*-heptane system were obtained at three temperatures, 40, 0, and −40 °F, from 20 up to 3272 psia. No lower temperatures could be examined for this system due to experimental limitations.

There have been a number of studies of the vapor-liquid equilibrium of the methane–*n*-hexane binary system, but only a few of these included dew-point data, and none reported dew-point data below 0 °C. Both phases were studied by Boomer and Johnson (*1*) at 25, 55, and 85 °C and by Poston and McKetta (*10*) over the range 100 to 340 °F. The lowest temperatures were studied by Shim and Kohn (*12*) in the range −110 to 150 °C, but they did not measure dew points below 0 °C.

For the methane–*n*-heptane system, earlier studies included those of Reamer et al. (*11*) from 40 to 460 °F and Kohn (*9*) from −130 to 271 °C, again with no dew-point data at the low temperatures. Chang et al. (*2*) of this laboratory reported measurements from 0 down to −100 °C for both phases. However, other correlative conformal solution studies in this University under T. W. Leland indicated that the *n*-heptane *K*-values were erroneous. This study has confirmed that surmise.

Experimental Method

The experimental equipment and technique have been reported in detail in earlier publications (*4, 5, 7*), which should be consulted for itemized information.

The modifications made to the equipment for the *n*-pentane calibration were also required in these studies. Again, *n*-hexane has a normal boiling point of 68.7 °C and *n*-heptane, 98.3 °C. For each case, the mixing valve, the sampling lines, and the thermal conductivity cell detector were kept at temperatures (80 and 115 °C, respectively) above these boiling points, to insure that the hydrocarbons would be in the gas phase.

The calibration curves exhibited the same type of behavior as the two previous studies, as could be expected from the principle of continuity. All of the calibration curves are shown in Figure 1. Again, the response curves were fit by a linear equation over most of the range of the investigation and by a third order polynomial for the curved regions, each by the least-squares method.

The sequence of the investigations was in the order of the carbon number, from higher temperatures to lower. For the *n*-hexane system, all isotherms were investigated up to 2000 psia; then a high-pressure methane cylinder (3500 psia) was installed, and the data above 2000 psia at 0 and −25 °C were taken. The 2000 psia points were also redetermined and were in agreement with the values determined previously. The *n*-heptane system was then investigated.

Materials

The *n*-hexane and *n*-heptane used in these investigations were donated by Phillips Petroleum Co. Both were research grade with a purity of 99.99 mol %. Methane with a purity of 99.97 mol % minimum, manufactured by Union Carbide Chemicals Corp., was purchased from IWECO. All materials were used without further purification.

Accuracy

The sources of errors include the fluctuations in system temperature, the error in the pressure measurement, the error in the calibration of the detector, and the error in the readout system. These errors were about the same magnitude reported in the previous papers, since the same equipment and experimental technique were used. The overall error in the dew-point data is either less than 2% or 0.00001 in mol fraction of *n*-hexane or *n*-heptane, depending on which is larger.

Experimental Results

The experimental data are presented in Tables I and II for the methane–*n*-hexane system and in Table III for the methane–n-heptane system. The results for the *n*-hexane system

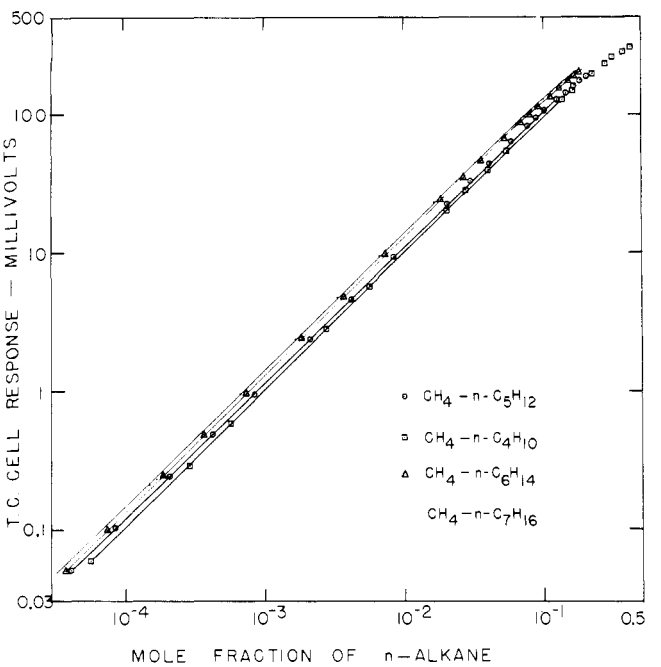

Figure 1. Calibration curves for methane–paraffin hydrocarbon binary systems *n*-butane through *n*-heptane

[1] Present address, Hudson Engineering Co., Houston, Tex.

Table I. Dew-Point Data for Methane–*n*-Hexane System

Press, psia	Mol fraction of *n*-hexane	Press, psia	Mol fraction of *n*-hexane	Press, psia	Mol fraction of *n*-hexane
T = 0.010 °C = 32.02 °F		T = −25.01 °C = −13.02 °F		T = −50.00 °C = −58.00 °F	
20.1	0.0442	20.1	0.0101	20.2	0.00159
25.1	0.0357	25.1	0.00821	25.2	0.00128
50.1	0.0185	50.1	0.00443	50.2	0.000657
100.1	0.0102	100.1	0.00243	100.2	0.000368
150.1	0.00734	150.1	0.00183	150.2	0.000287
200.1	0.00604	200.1	0.00153	200.2	0.000243
300.1	0.00472	300.1	0.00128	300.2	0.000225
400.1	0.00434	400.1	0.00121	400.2	0.000245
600.	0.00422	600.	0.00137	600.	0.000406
800.	0.00451	800.	0.00180	800.	0.000744
1000.	0.00535	1000.	0.00241	1000.	0.00149
1200.	0.00657	1200.	0.00368	1200.	0.00387
1400.	0.00834	1400.	0.00584	1400.	0.00987
1600.	0.0109	1600.	0.00948	1500.	0.0129
1800.	0.0151	1800.	0.0156	1600.	0.0159
2000.	0.0203	2000.	0.0248	1700.	0.0184
2200.	0.0308	2200.	0.0356	1804.[a]	0.0216
2400.	0.0435	2300.	0.0407		
2600.	0.0634	2332.	0.0426		
2675.[a]	0.0710	2337.[a]	0.0436		
T = −63.00 °C = −81.40 °F		T = −70.00 °C = −94.00 °F		T = −75.10 °C = −103.18 °F	
20.2	0.000505	50.3	0.000117	19.9	0.000152
25.2	0.000411	100.3	0.000076	25.0	0.000115
50.2	0.000219	150.3	0.000068	50.0	0.000073
100.2	0.000132	200.3	0.000065	100.0	0.000051
150.2	0.000112	300.3	0.000076	150.0	0.000045
200.2	0.000097	400.3	0.000095	200.0	0.000048
300.2	0.000106			300.0	0.000061
400.2	0.000122			400.0	0.000081
600.	0.000202			500.0	0.000107
800.	0.000598			600.	0.000168
1000.	0.00270			700.	0.000360
1200.	0.00823			800.	0.00211
1400.	0.0118			900.	0.00428
1443.[a]	0.0128			1000.	0.00565
				1057.[a]	0.00636
T = −80.00 °C = −112.00 °F		T = −82.65 °C = −116.77 °F			
20.1	0.000095	20.0	0.000076		
25.1	0.000068	25.0	0.000040		
100.1	0.000036	100.0	0.000030		
300.1	0.000030	300.0	0.000012		
500.1	0.000068	499.6	0.000093		
600.	0.000170	600.	0.000186		
675.	0.000433	638.[b]	0.000389		
692.[b]	0.000607	645.	0.000423		
700.	0.00102	650.	0.000413		
708.[a]	0.00118	655.	0.000391		
		660.	0.000313		
		665.	0.000153		

[a] Critical. [b] L_1-L_2-G.

Table II. Phase Behavior for Methane–*n*-Hexane System in Vicinity of Critical Point of Methane

Temp, °C	Press, psia, for L_1-L_2-G[a]	Mol fraction of *n*-hexane in vapor-phase G	Critical press, psia, for L_1-L_2
−77.24	755[b]	0.00237	986
−80.00	692	0.000607	883
−82.65	638	0.000389	770
−86.92	559	0.000163	624
−90.69	495.3[c]	0.000054	495.3

[a] L_1 = methane-rich liquid phase, L_2 = *n*-hexane-rich liquid phase, G = vapor phase, and L_1-L_2-G = three-phase condition. [b] Upper end of L_1-L_2-G line and also critical point of L_1-G. [c] Lower end of L_1-L_2-G line, lower critical solution point, and critical point of L_1-L_2.

are shown in Figures 2–7; the *n*-heptane system is represented by Figures 8–11.

Methane–*n*-Hexane System

The pressure-composition behavior is shown in Figure 2 for the high-temperature portion of the investigation, 0 down to −75 °C. The behavior at the higher pressures is almost linear in Figure 2. An expanded scale is used in Figure 3 to present the details of the behavior in the low-temperature region of investigation, −50 down to −82.65 °C. This figure shows the intrusion of two liquid phases into the system; details are tabulated in Table II. In other ways this figure is continuous with the similar figures for the *n*-butane and *n*-pentane systems (*6*). The S-type shape of the critical isotherm in Figure 3 should be observed.

Table III. Dew-Point Data for Methane–*n*-Heptane System

Press, psia	Mol fraction of *n*-heptane	Press, psia	Mol fraction of *n*-heptane	Press, psia	Mol fraction of *n*-heptane
T = 40.00 °F = 4.440 °C		T = 0.00 °F = −17.78 °C		T = −40.00 °F = −40.00 °C	
20.3	0.0154	20.2	0.00376	19.8	0.000618
25.3	0.0125	25.2	0.00291	25.0	0.000485
50.3	0.00656	50.2	0.00157	50.0	0.000285
100.3	0.00364	100.2	0.000872	100.0	0.000160
200.3	0.00223	200.2	0.000584	200.0	0.000109
400.3	0.00165	400.2	0.000501	400.0	0.000129
600.	0.00164	600.	0.000584	600.	0.000166
800.	0.00187	800.	0.000735	800.	0.000287
1000.	0.00229	1000.	0.00107	1000.	0.000546
1250.	0.00315	1250.	0.00180	1250.	0.00140
1500.	0.00446	1500.	0.00313	1500.	0.00360
1750.	0.00644	1750.	0.00555	1750.	0.00811
2000.	0.00940	2000.	0.00934	2000.	0.0138
2250.	0.0136	2250.	0.0140	2250.	0.0194
2500.	0.0200	2500.	0.0213	2500.	0.0256
2750.	0.0303	2750.	0.0319	2675.[a]	0.0310
3000.	0.0438	3000.	0.0449		
3250.	0.0668	3005.[a]	0.0458		
3272.[a]	0.0690				

[a] Critical.

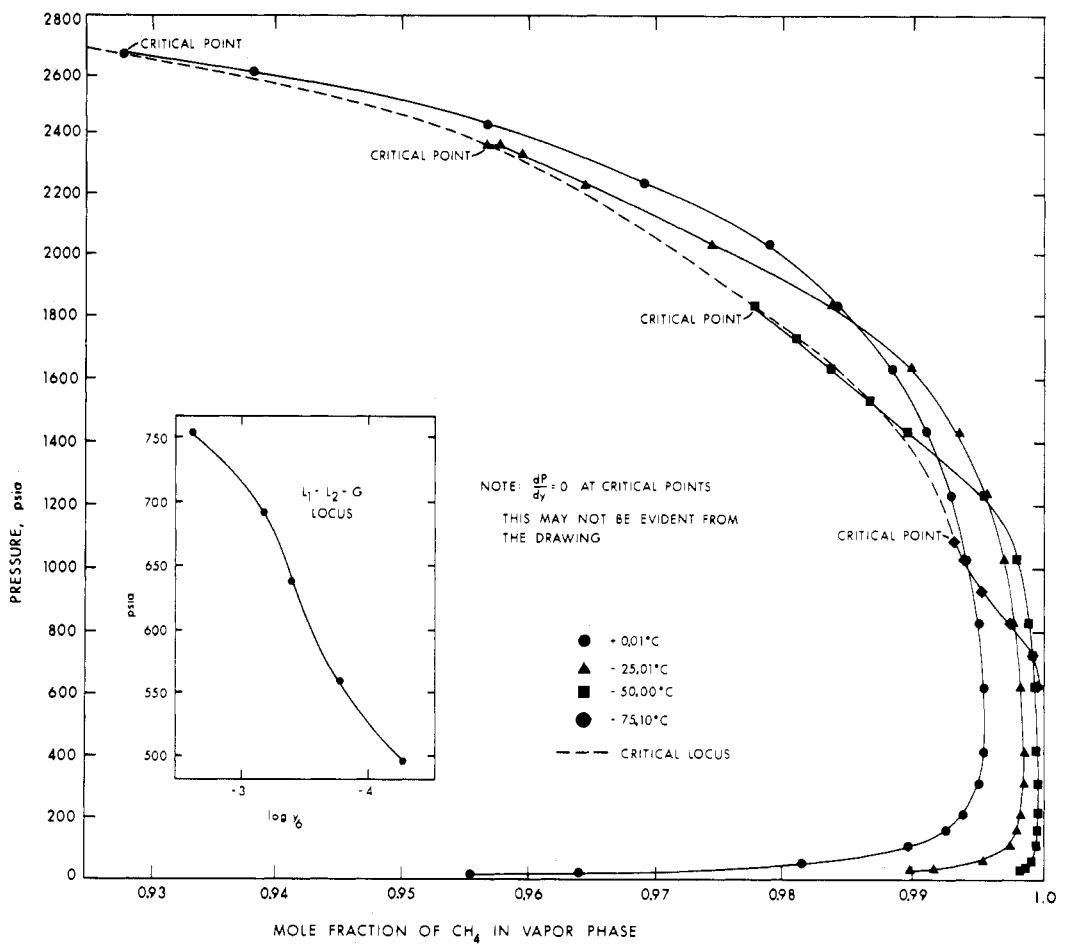

Figure 2. Isothermal dew-point behavior for methane–*n*-hexane system at 0, −25, −50, and −75.10 °C

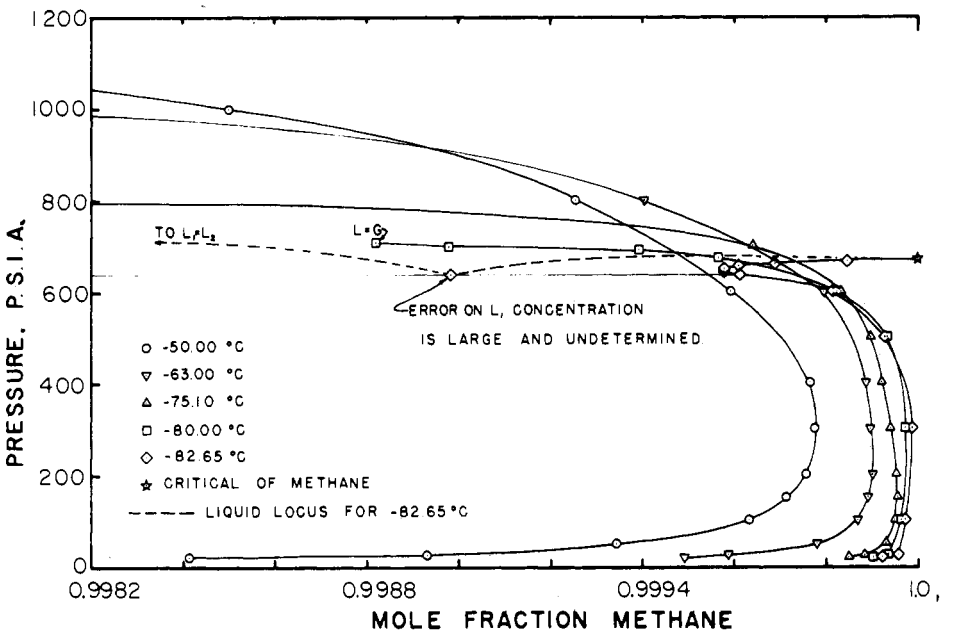

Figure 3. Isothermal dew-point behavior for methane–*n*-hexane system in low-temperature region. Note magnitude of mol fraction

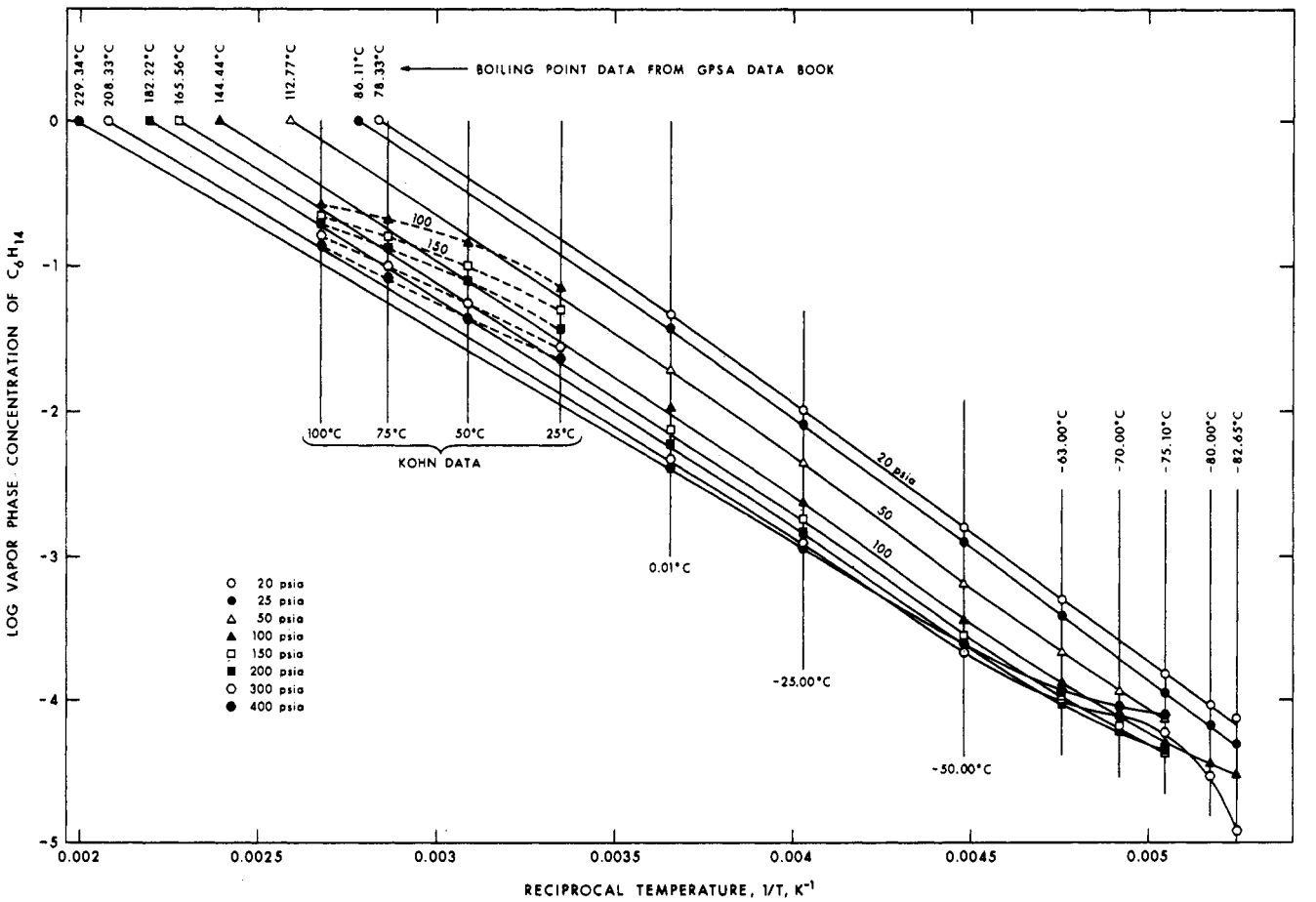

Figure 4. Isobaric dew-point behavior for methane–*n*-hexane system in low-pressure regions

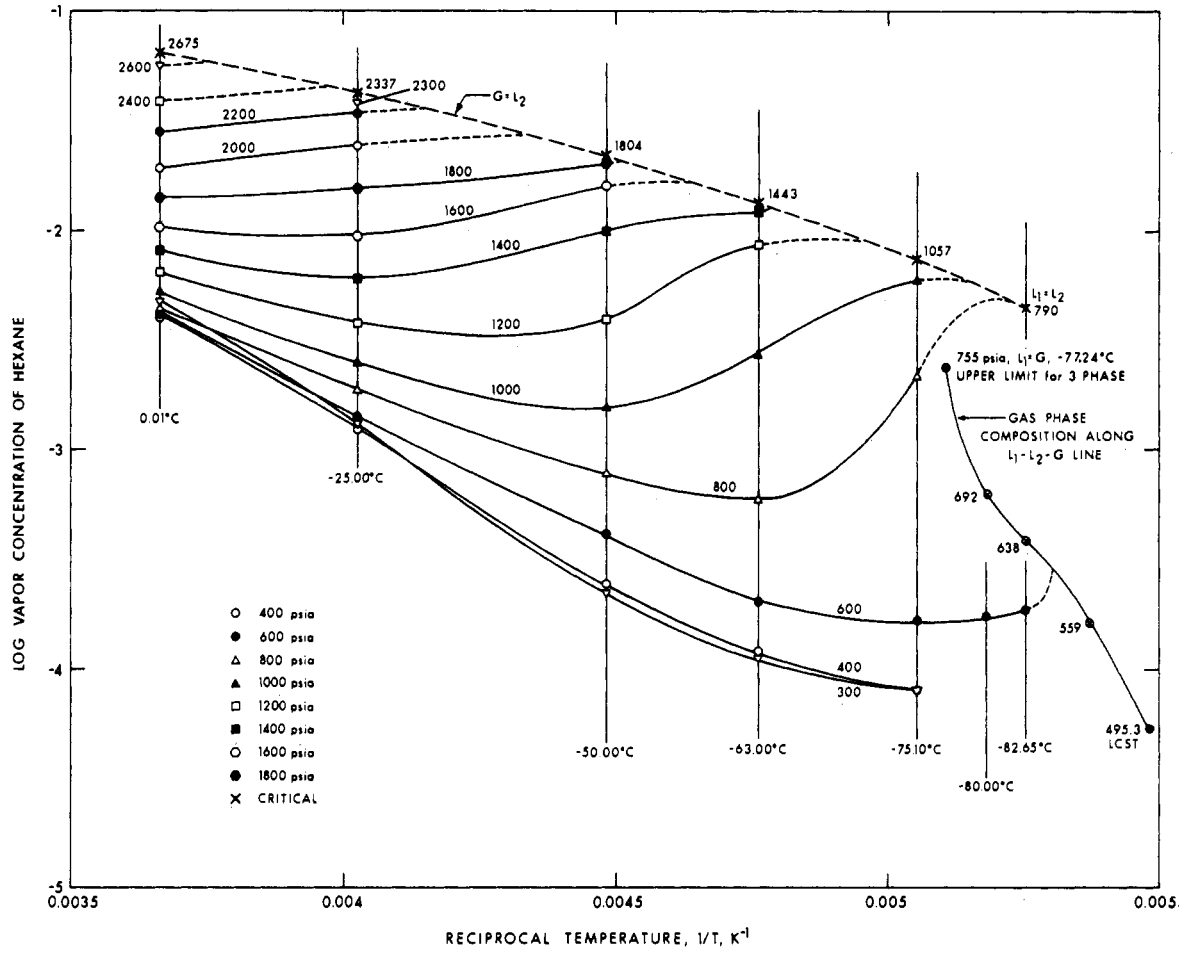

Figure 5. Isobaric dew-point behavior for methane–*n*-hexane system in high-pressure regions

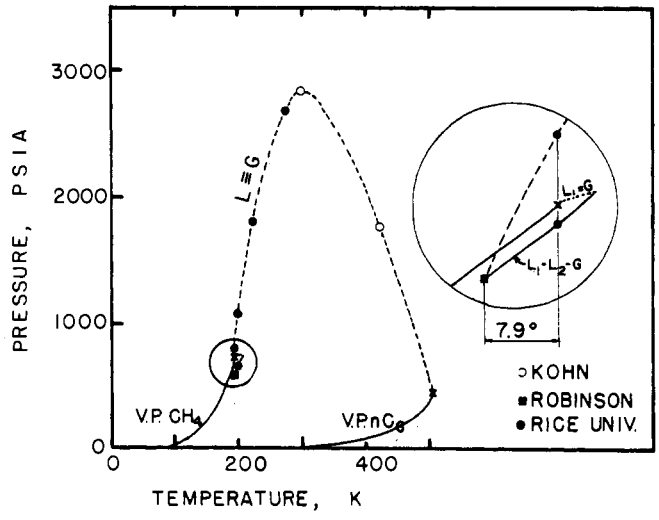

Figure 6. Phase diagram for methane–*n*-hexane system

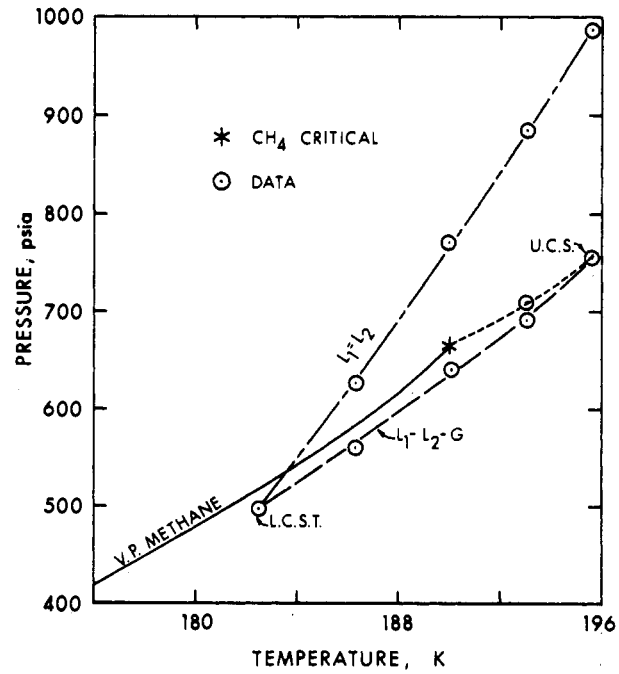

Figure 7. Details of three-phase region near critical point of methane for methane–*n*-hexane system

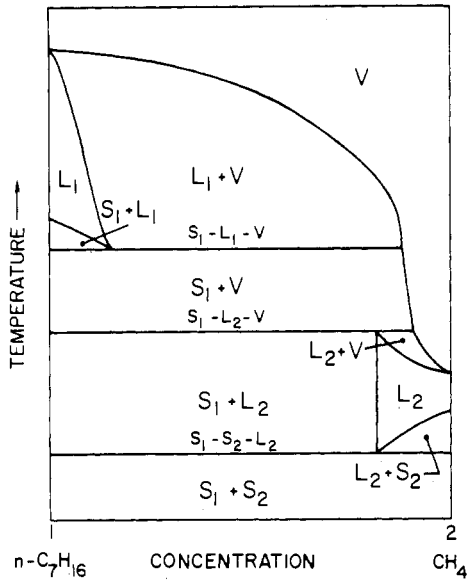

Figure 8. Qualitative phase behavior for methane–*n*-heptane system at 200 psia

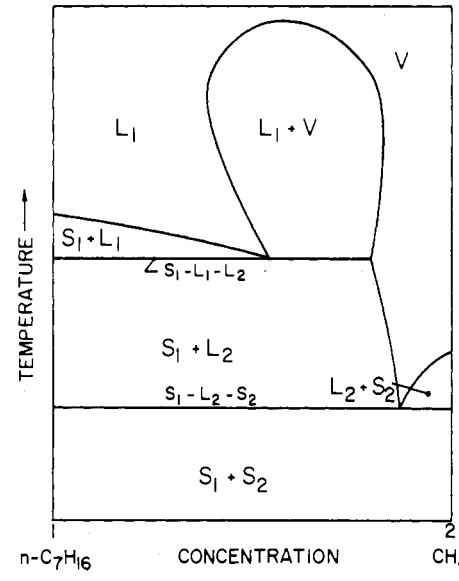

Figure 10. Qualitative phase behavior for methane–*n*-heptane system at 1000 psia

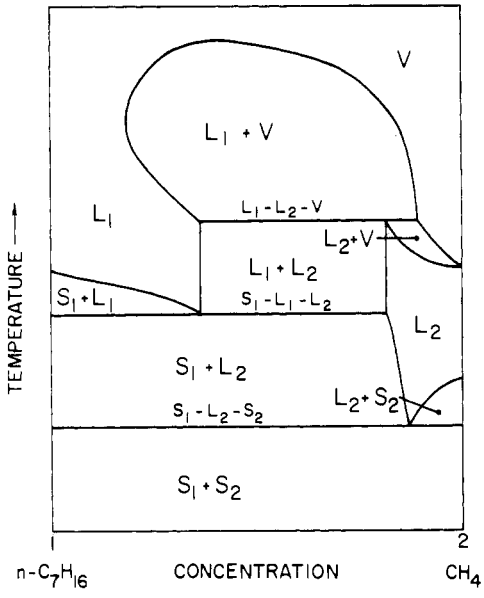

Figure 9. Qualitative phase behavior for methane–*n*-heptane system at 600 psia

Figures 4 and 5 present the isobaric behavior of the dew point for the methane–*n*-hexane system for low- and high-pressure regions. In the construction of Figure 4, the vapor-pressure points (boiling-point temperatures) for *n*-hexane provided the limits of the isobars.

A pressure vs. temperature phase diagram is shown in Figure 6, with the details of the three-phase region shown in Figure 7. The three-phase region (two liquid phases) was observed over the range −90.69 up to −77.24 °C. The lower critical solution temperature, −90.69 °C or 182.46 K, compares favorably with the 182.6 K for the LCST determined by Davenport and Rowlinson (*8*). No direct comparison with other vapor-liquid equilibrium data is possible, since none exists. The extrapolation of the dew-point data to the boiling points, shown in Figure 4, is smooth. The critical locus in Figure 6 shows a match between these data and those reported by Shim and Kohn (*12*).

Methane–*n*-Heptane System

Since only three isotherms were measured for this system, a fully detailed analysis is not possible. However, the data do show that the principle of continuity applies to the paraffin hydrocarbon phase behavior.

The information obtained in this study and the application of the phase rule led to Figures 8–10, which are temperature vs. concentration diagrams at 200, 600, and 1000 psia. These figures are qualitative and not quantitative; they illustrate the intrusion of the second liquid phase.

The pressure-composition behavior for the three isotherms studied is shown in Figure 11. Note that the same data are shown on two different composition scales for pressures below 1800 psia. This same smoothness and continuity of behavior has been observed in all of these dew-point studies (*6*).

K-Values

These data have been combined with data from other investigations for the bubble-point values to yield tentative *K*-values for both systems (*3*). These *K*-values were prepared to provide guidelines for engineering calculations only, and in no way should these *K*-values be regarded as experimental data.

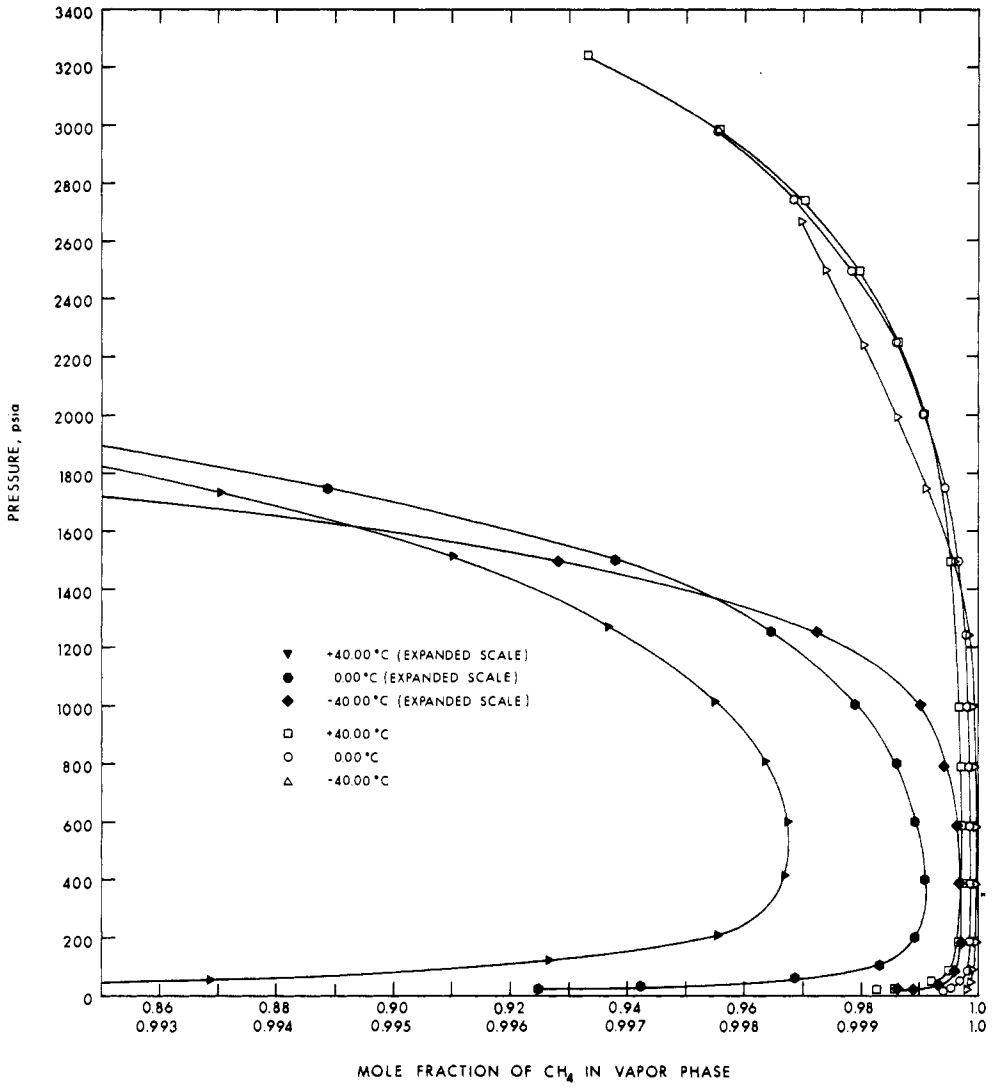

Figure 11. Isothermal dew-point behavior for methane–*n*-heptane system at +40, 0, and −40 °C. Note expanded scale for low-pressure portion of data

Literature Cited

(1) Boomer, E. H., Johnson, C. A., *Can. J. Res.*, **16B**, 395 (1938).
(2) Chang, H. L., Hurt, L. J., Kobayashi, R., *AIChE J.*, **12**, 1212 (1966).
(3) Chappelear, P. S., *Proc. Gas Proc. Assoc.*, **53**, 26 (1974).
(4) Chen, R.J.J., Chappelear, P. S., Kobayashi, R., *J. Chem. Eng. Data*, **19**, 53 (1974).
(5) Chen, R.J.J., Chappelear, P. S., Kobayashi, R., *ibid.*, p 58.
(6) Chen, R.J.J., Chappelear, P. S., Kobayashi, R., paper F 6-1, preprints Vol IV, GVC/AICHE Joint Meeting, Munich Germany, Sept. 17–20, 1974.
(7) Chen, R.J.J., Ruska, W.E.A., Chappelear, P. S., Kobayashi, R., *Adv. Cryog. Eng.*, **18**, 202 (1972).
(8) Davenport, A. J., Rowlinson, J. S., *Trans. Faraday Soc.*, **59**, 78 (1963).
(9) Kohn, J. P., *AIChE J.*, **7**, 514 (1961).
(10) Poston, R. S., McKetta, J. J., *J. Chem. Eng. Data*, **11**, 362 (1966).
(11) Reamer, H. H., Sage, B. H., Lacey, W. N., *ibid.*, **1**, 37 (1956).
(12) Shim, J., Kohn, J. P., *ibid.*, **7**, 3 (1962).

Received for review August 11, 1975. Accepted December 29, 1975. Financial support provided primarily by the Gas Processors Association, with secondary support from the National Science Foundation, the American Gas Association, and Columbia Gas Systems Service Corp.